Companding Techniques for High Dynamic Range Audio CODEC Receiver Path

by

Yunjie Ma

S.B. EE, MIT (2008)

Submitted to the Department of Electrical Engineering and Computer Science
in partial fulfillment of the requirements for the degree of

Master of Engineering in Electrical Engineering and Computer Science

at the

MASSACHUSETTS INSTITUTE OF TECHNOLOGY

June 2009

Author .....
Department of Electrical Engineering and Computer Science
May 22, 2009

Certified by.....
Guoqing Miao
Director of Engineering, Qualcomm
VI-A Company Thesis Supervisor

Certified by.....
Vladimir Stojanovic
Assistant Professor of Electrical Engineering
M.I.T. Thesis Supervisor

Accepted by .....
Arthur C. Smith
Chairman, Department Committee on Graduate Theses

Companding Techniques for High Dynamic Range Audio CODEC Receiver Path

by

Yunjie Ma

Submitted to the Department of Electrical Engineering and Computer Science
on May 22, 2009, in partial fulfillment of the
requirements for the degree of
Master of Engineering in Electrical Engineering and Computer Science

Abstract

In this thesis, an audio CODEC receiver path has been modified by the addition of companding techniques. Companding compresses the input signal and expands the output signal according to the input power strength such that additional noise from the system is suppressed while the signal content is maintained. As the compression level is varied according to the input signal strength, transients occur at the output of the system. Sudden changes in the compression level cannot be processed instantaneously and generate transients in the output. The thesis first statically demonstrates that companding can increase the signal to noise ratio and improve the dynamic range of the audio CODEC Rx path by up to 18 dB. Further, two compensation techniques are analyzed in attempt to reduce the companding transients. The results show that transients in the output are reduced on average by 60% when using either compensation technique.

VI-A Company Thesis Supervisor: Guoqing Miao
Title: Director of Engineering, Qualcomm

M.I.T. Thesis Supervisor: Vladimir Stojanovic
Title: Assistant Professor of Electrical Engineering

Acknowledgments

I am grateful to MIT, the Course VI department, and the VI-A program for providing me the opportunity to perform my Master of Engineering thesis at Qualcomm.

I would like to thank Guoqing Miao, Song Wang, and Derick Hugunin at Qualcomm for their insight, support, and advice on my thesis. Our meetings always gave me ideas even when there seemed to be no other method.

Thank you Professor Vladimir Stojanovic for your guidance throughout my thesis project.

To my friends, and especially Lawrence, thank you for always being there for me.

To my family, thank you for your guidance, support, and love for the past 22 years.

Contents

List of Figures

List of Tables

Chapter 1

Introduction

This thesis aims to improve the audio CODEC receiver path of the Marimba chip, part of the Snapdragon chipset with features for Bluetooth, audio codec + touch screen, and FM transceiver/receiver. The thesis analyzes different companding systems to improve the dynamic range of the CODEC receiver path. Companding compresses the input signal and expands the output signal to keep the signal level above the noise level during processing. The static effects, improvements in SNR, and dynamic effects, transients caused by input power changes, of these companding techniques are analyzed in this paper.

The thesis is divided into the following chapters.

Chapter 2 describes existing Marimba CODEC receiver path, a system that converts a digital audio input into an analog signal to be played on the speaker or headset of a cellular phone. The goal of this thesis is to improve the signal to noise ratio (SNR) of the system for small input signals. Conventional analog techniques would consume too much power and therefore cannot be used to improve the SNR. Instead, the thesis will focus on different companding techniques.

Chapter 3 describes the method of companding, a signal processing technique used to increase the dynamic range of systems. The formation of the word companding comes from the words compressing and expanding. Companding compresses the dynamic range of input signal and expands the dynamic range of the output signal so that the noise is suppressed while the signal is maintained. Since first patented by

A.B. Clark in 1928, companding has had a variety of applications in communication systems, audio recordings, and signal processing, see [1], [8], and [14]. Chapter 3 explains in detail the two type of companding systems that exist: instantaneous companding and syllabic companding.

Chapter 4 describes how the thesis applies syllabic companding to the receiver path. Three additional system blocks are added to the receiver path: a root mean squared (RMS) power detector, a variable gain amplifier, and a variable gain attenuator. The amplifier acts as the compressor and the attenuator acts as the expander. The placement of the compressor and the expander minimizes the effects of the delta sigma quantization noise and the DCT (direct charge transfer) analog noise.

Chapter 5 describes the transients that are inadvertently caused by the new companding system. These transients are formed when a change in the input signal power level is detected. The change is not processed instantaneously by the companding system, causing transients to form. Different methods to reduce the transients are discussed in this chapter. These compensation techniques include adding an additional delay in the expander control path and manipulating the control path to change the signals at more optimal times.

Chapter 6 describes the first set of simulations: static simulations. The transients are first ignored to study SNR improvements in the audio CODEC receiver path with companding. By keeping the compressor and expander gain levels constant, the transients disappear. The simulations test the companding system with various input amplitudes, compression levels, sampling frequencies, and over-sampling ratios (OSR).

Chapter 7 describes the dynamic simulations of the audio CODEC receiver path with companding. In addition to the original companding system, these simulations test the two compensation methods discussed in Chapter 5. The transients are produced in the output by changing the gain level signal which controls the compressor and the expander.

This thesis shows that companding increases the dynamic range of audio receiver path by up to 18 dB. Further, the compensation methods discusses are able to reduce

the transients caused by syllabic companding by 60% on average.

Chapter 2

Marimba audio CODEC receiver path

The audio codec lies on the Marimba chip, part of Qualcomm's Snapdragon chipset offering for cellular phones. The thesis focuses on the receiver path of the codec, which converts a pulse code modulated (PCM) stream (16-bit to 24-bit) input into an analog signal to be supplied directly to the headphone or ear piece. Since the output is an audio signal, the inband frequencies for the system are in the audible range of 20 Hz to 20,000 KHz.

Figure 2-1 depicts the block diagram for the receiver path.

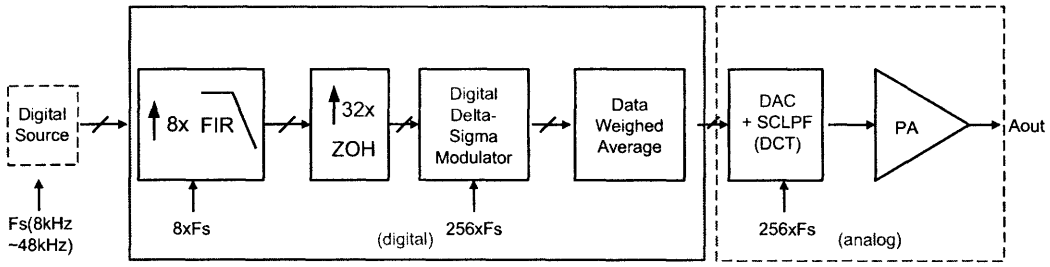

Figure 2-1: The CODEC receiver path converts an audio digital source into an analog output. The system first upsamples the input signal, modulates it into a 4-bit signal, and converts it into an analog signal while filtering out the high frequency noise. The block diagram is depicted in the figure.

2.1 Description of the Rx path

The input is a PCM stream digital input encoded in 16-bit to 24-bit with a sampling frequency between 8 KHz and 48 KHz. In the receiver path, the input signal is first upsampled by 8x. To conserve power consumption, upsampling is performed by three sets of upsampling and interpolation blocks, increasing the OSR by 2 at each step. The three interpolation filters are all FIR low-pass filter (LPF). Because of the low sampling frequency, the first filter can afford to be calculation intensive, with an order of 64. As the sampling frequency doubles, the filter orders become smaller; The second and third filter have orders of 19 and 11 respectively. The interpolation filters were originally designed to compensate for in-band attenuation caused later by the zero order hold block and the direct charge transfer (DCT) block.

The signal is then upsampled again by a zero order hold (ZOH). The ZOH can be set with an OSR of 8x, 16x, or 32x. The total OSR of the receiver path is 64x, 128x, or 256x. The oversampling prepares the signal for the delta sigma modulator. A higher OSR results in less quantization noise shaped into the inband but at the cost of higher power consumption.

The digital delta sigma ($\Delta\Sigma$) modulator then converts the signal into a four bit stream. The quantization noise added by the conversion is shaped by the $\Delta\Sigma$ modulator feedback loop such that its spectrum is concentrated at high frequencies, with respect to the the current sampling frequency. The transfer function is given in Equation 2.1 for the constants

$$\begin{aligned} a_1 &= 1 \\ a_2 &= 1.1875 \\ a_3 &= 2a_2 \end{aligned}$$

and nbits being the number of bits in which the input is encoded.

$$H_{\Delta\Sigma}(z) = \frac{\frac{a_1}{2^{nbits-5}} z^{-2}}{1 + (\frac{a_3}{2} - 2)z^{-1} + (1 - \frac{a_3 - a_2}{2})z^{-2}} \tag{2.1}$$

The now 4-bit signal is then converted to analog by a data weighed average (DWA) and a direct charge transfer (DCT). The DWA converts the 4-bit or 16 unit signal into 18 units by adding two randomly generated values to the two additional units. The purpose of the DWA is to randomize the signal harmonic distortion and noise tones generated by the DAC element mismatch in order to push them out of the signal band.

The DCT acts as the digital to analog converter (DAC) and a low pass filter. In simulations, the DCT is a first order IIR filter with the cutoff frequency depending on the OSR to filter out the $\Delta\Sigma$ quantization noise accordingly. The DCT is the first analog block in the system and adds analog noise to the signal. In simulation, this noise is modeled to be at -100 dBFS and -90 dBFS.

Lastly, the signal is amplified by a power amplifier (PA). The effects of the PA, including the analog noise added by the PA, are mostly ignored in this thesis. The PA contributes to the companding techniques because it can attenuate the signal at 1.5 dB steps, with an error up to ± 0.5 dB. The ability to attenuate the signal is crucial to the companding techniques that will be discussed.

2.2 Rx path noise sources

There are four noise sources in the current system. First, PCM quantization noise exists in the digital input signal. The quantization noise is inversely proportional to the number of bits in which the input is encoded. For example, a signal that is encoded into 16 bits can have a maximum SNR of only 98 dB. The next noise source is the $\Delta\Sigma$ quantization noise, which is formed when the upsampled input is converted into 4 bits. The feedback loop in the $\Delta\Sigma$ modulator shapes the quantization noise such that it is concentrated mainly at high frequencies, with respect to the oversampled sampling frequency. At low F_s and OSR, the $\Delta\Sigma$ quantization noise may still exist in the inband, between 20 Hz and 20 KHz, see Figure 2-2.

Lastly, analog noise is introduced by the DCT and the PA. In simulation, the DCT analog noise is simulated as either -100 dBFS or -90 dBFS white Gaussian noise. The

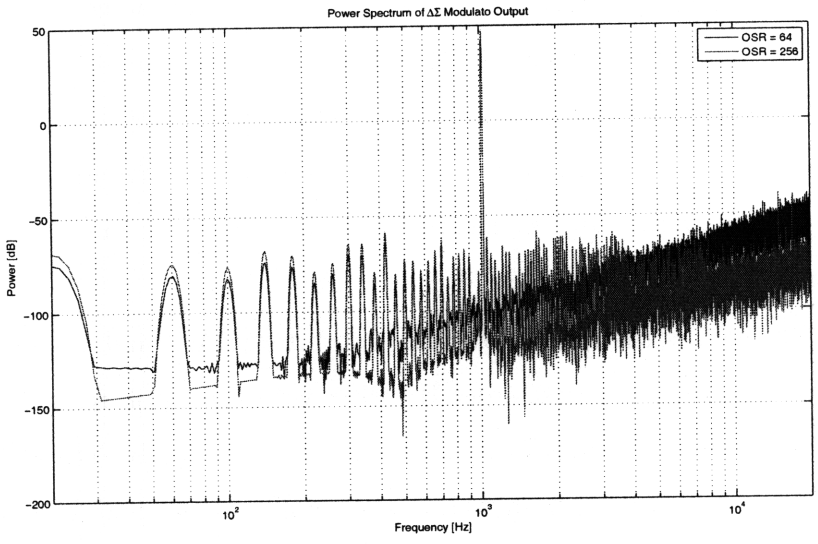

Figure 2-2: The inband, 20 Hz to 20 KHz, power spectrum at the output of the $\Delta\Sigma$ modulator is plotted. The $\Delta\Sigma$ modulator is simulated with an OSR of 64x and 128x. The figure shows that the $\Delta\Sigma$ quantization noise is much higher when the OSR is at 64x.

PA analog noise is ignored in this project.

2.3 Rx path improvements

The goal of the thesis is to reduce the effects of the dominant noise source, the analog DCT noise. Conventional analog techniques require twice the amount of power just to reduce the DCT noise by 3 dB. In the current implementation of the receiver path, the change in the DCT would require approximately an additional 2.2 mWatts. The thesis is interested in other methods, that is companding techniques, to save power while reducing the effects of the DCT noise. The addition of companding requires additional digital components, which are much more energy efficient. Currently, the digital interpolation filters, which are more calculation intensive than the digital blocks required for companding, consumes only 180 μWatts of power.

Chapter 3

Companding basics

A companding system compresses the signal at input and expands the signal at output in order to keep the signal level above the noise level during processing. In other words, companding amplifies small inputs so that the signal level is well above the noise floor during processing. At the output, the original input signal is then restored by a simple attenuation. Companding increases the SNR when the input signal is low and therefore reduces the effect of a system's noise source.

3.1 History and applications

The concept of companding was first patented by A.B. Clark at AT&T in 1928. The purpose of the patent was to adaptively transmit images through a noisy medium such that the received image has tone values similar to the image transmitted [1]. Since then, companding has been developed for numerous other applications such as audio transmission and recording, communication systems, and signal processing [14][8]. The μ-Law, for example, applies a logarithmic formula to audio or speech signals such that the transmit signals has a smaller number of bits. The logarithmic formula compresses the signal by allocating more bits or quantization levels to smaller values to reduce the signal to quantization noise ratio, which in general increased as the amplitude of the signal decreased [10].

New variations of companding for transmission and communications have been

proposed using the hyperbolic tangent function [2]. Used for OFDM signals, the hyperbolic tangent can reduce the magnitude of the signal peaks to increase the efficiency in transmission. In all the examples cited above, only a simple compression algorithm is required because the transmission channel is modeled as additive noise. If convolutions occurred within the channel, as in companding for signal processing, then compensation methods would be required to reduce the effects of transients, see Chapter 5.

Recent applications of companding have been developing in the fields of analog and digital signal processing. Tsividis first proposed using companding in analog signal processors in [14]. Unlike previous companding techniques where the transmitter and the receiver are geographically different locations, the compressor and expander for a signal processor can be placed on the same chip, introducing the concept of syllabic companding: the compression level is known to both the compressor and the expander and can be determined by the average value of the input rather than the instantaneous value of the input. The concept is demonstrated in [14] for a second-order high Q bandpass filter. It was found that transients occur within companding signal processors [13] and various compensation methods are discussed in Chapter 5.

Using companding on signal processors has the additional benefit of lower power dissipation for a required signal to noise ratio. In [15], it is shown that to increase the SNR requirements of an analog system by 3 dB requires twice the capacitance area and double the power dissipation. If companding is employed, then the necessary SNR can be met without such a large increase in chip size and power consumption.

3.2 The benefits of companding

For a generic signal processor, the output is comprised of three components: signal, noise and distortion. If the processor is linear, then Figure 3-1 shows the relationship between the input and the output components as the input level increases. The output signal is proportional to the input level while noise is generally independent of the input. At high input levels, the linearities of the system can no longer be

maintained, and distortion occurs [13].

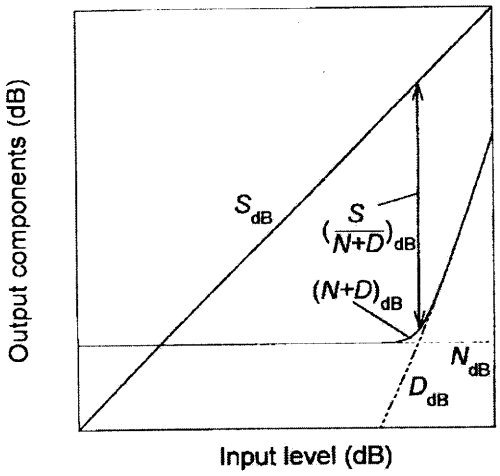

Figure 3-1: The input-output relationship of a typical analog signal [13].

A plot of the input level versus the signal to noise and distortion ratio (SNDR) is shown in Figure 3-2(a). The plot demonstrates that the dynamic range of the system is limited when the output SNDR is required to be above a given level. To increase the dynamic range, it is possible to redesign the processor such that the noise level is lowered. However, a decreased noise level can only increase the dynamic range by a small amount, see Figure 3-2(b). For a wider acceptable dynamic range, companding must be implemented, see Figure 3-2(c).

Companding works by compressing the dynamic range of the signal at the input and expanding the dynamic range at the output. Compression occurs when small signals are amplified and large signals are attenuated. Thus, the signal strength can be kept significantly higher than any noise that may be introduced into the system, even at low input power. At output, the expander then restores the input signal, while keeping the signal power above the noise level and increasing the SNDR of the signal [5]. Companding affects the signal differently depending on the signal; this can be seen in Figure 3-3.

There are two types of companding techniques, instantaneous and syllabic com-

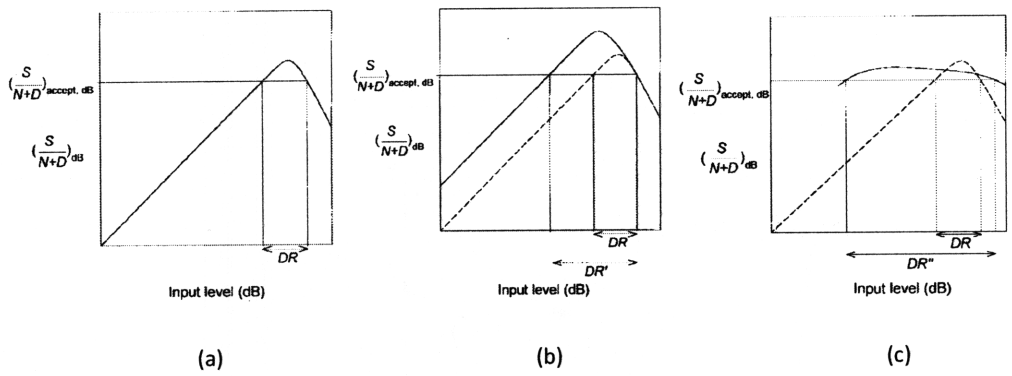

Figure 3-2: The three plots demonstrate the input to SNDR relationships for an analog signal processor a) without any changes, b) with a decreased noise floor, and c) with a companding system [13].

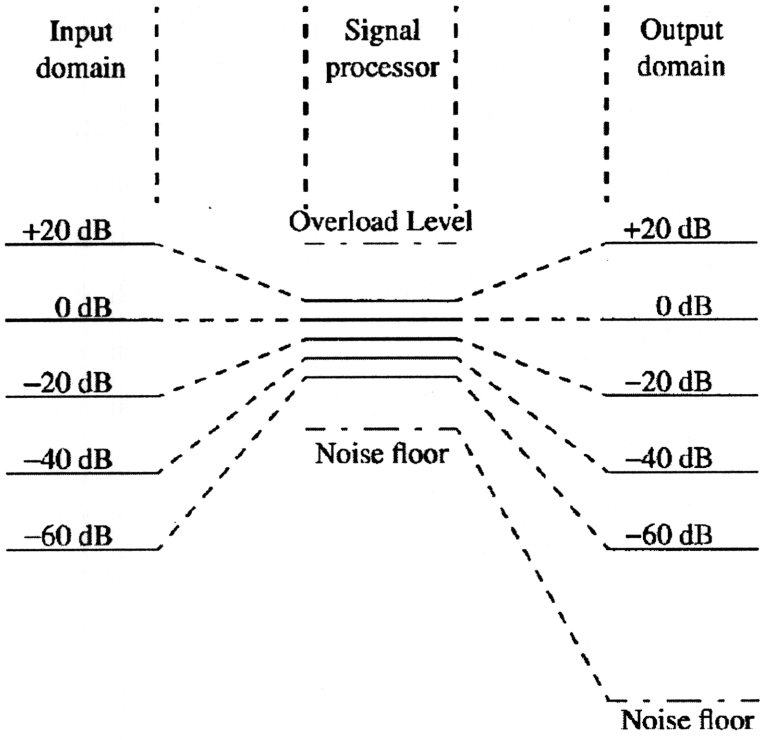

Figure 3-3: Companding compresses the input domain such that the signal level stays above the noise floor during processing. The output is then expanded to match the input domain while keeping the noise level low [13].

panding. The two techniques differ on how the signal is compressed and expanded. Instantaneous companding compresses the input signal according to the instantaneous input level. Syllabic companding compresses depending on the average strength, for example the envelope or the peak, of the input signal [12].

3.3 Instantaneous companding

Instantaneous companding is a memoryless system: signals are compressed according to the current values in the system, not the past values. For example, the μ-law algorithm is an example of instantaneous companding. The compressed signal is calculated by Equation 3.1a and Equation 3.1b.

$$\gamma(\nu) = \frac{log_2(1+\mu\nu)}{log_2(1+\mu)}, \nu \geq 0 \tag{3.1a}$$

$$\gamma(\nu) = -\gamma(-\nu), \nu < 0 \tag{3.1b}$$

A higher μ corresponds to a higher compression level. The μ-law behavior, with $\mu = 255$ is plotted in Figure 3-4. From the figure, it can be seen that small values of ν are amplified while large values of ν are attenuated [6].

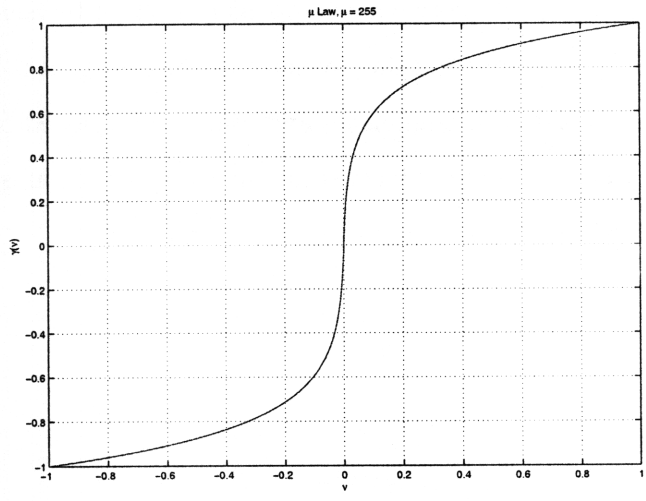

Figure 3-4: The μ-law is a compression method that is used in instantaneous companding. This figure plots the input-output relationship when μ is set to 255.

3.4 Syllabic companding

Unlike instantaneous companding, the compressor and expander in syllabic companding depends on the average power level of the signal [13]. Figure 3-5 is a basic diagram of syllabic companding. The additional E block detects the strength of input signal u, and generates the signal U, the control signal for the compressor and expander.

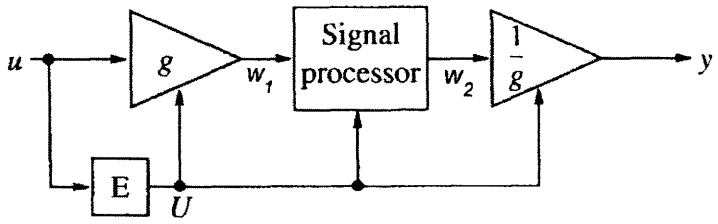

Figure 3-5: The block diagram shows that compression and expansion in syllabic companding depends on the average input power, detected by block E [13].

The signal U is a measure of the average power input. A low U signal translates to a high g signal and vice-versa. The value of g indicates the level of compression and expansion, changing dynamically depending on previous values of the input signal.

Letting u be the input, y be the output, and w_1 and w_2 be signals within the signal processor, Figure 3-6 plots what happens to each of the signals during syllabic companding. The gain signal, g, is high when the average input is low and is low when the average input is high. The signals w_1 and w_2 are compressed based on the average input level and thus remain mostly constant. The output signal is regenerated by the expander and thus appears similar to the input signal [13].

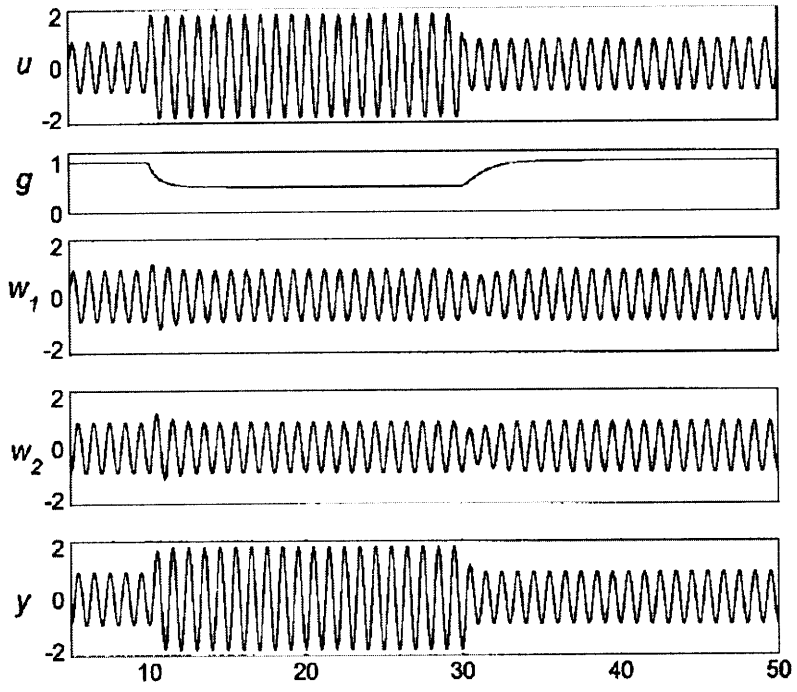

Figure 3-6: When the power of the input signal, x, increases, the gain signal, g, decreases causing compression to occur. Within the processor, w_1 and w_2 appear to be stay mostly at a constant power level while the output signal, y, is expanded to reflect the original input signal [13].

Chapter 4

Apply companding to the audio CODEC Rx path

The goal of the thesis is to increase the dynamic range of the CODEC receiver path. Companding will cause system to have higher signal-to-noise ratios when the input signal strength is small and will then expand the dynamic range of the system.

This thesis will apply syllabic companding to the audio CODEC receiver path. Instantaneous companding compresses the input signal according to the value of the signal at every sample point, causing the compression level to constantly fluctuate. However, as Chapter 5 will explain, the compression level should be kept constant as much as possible such that the transients formed by companding are minimized. Syllabic companding changes the compression level only when the average power of the input signal changes and will cause less transients in the CODEC receiver path.

Two examples of applying syllabic companding to audio systems are cited in [3] and [9]. In [3], Palaskas and Tsividis successfully decreased the noise measured at the output of a second order frequency filter by 20 dB. In [9], companding was applied to the ADC (Analog to Digital Converter) of a hearing aid in order to reduce the power consumption requirements by more than 60% compared to previous work. In both examples, the dynamic transients caused by companding were eliminated using the method described in Appendix Section A.1.

The block diagram of Rx path with basic syllabic companding is shown in Figure 4-

1.

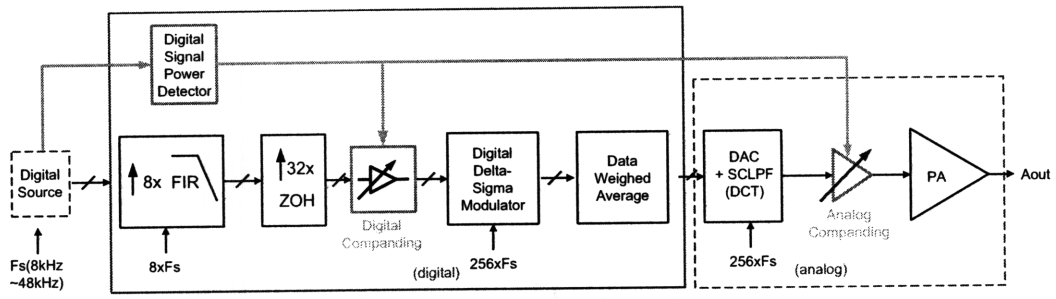

Figure 4-1: The audio receiver path with the addition of a detector, compressor and expander.

A root mean squared (RMS) power detector is connected to the input signal, which generates a gain level signal that controls the level of companding. When the input power is low, the companding gain level is high and when the input power is high, the companding gain level is low.

A digital variable amplifier is the compressor and is placed between the zero order hold (ZOH) and the delta sigma modulator. The amplifier is a compressor because it amplifies when the input signal is small.

An expander, or an analog variable attenuator, is added after the direct charge transfer (DCT). Working opposite of the compressor, the expander attenuates its input according to the companding gain level signal. Fortunately, the attenuator functionalities is already present in the power amplifier, eliminating the need to design a new analog component which would have increased power consumption. The power amplifier has the ability to attenuate the signal in 1.5 dB steps. The drawback of using the power amplifier is that the attenuation level can be controlled with an accuracy of ± 0.5 dB. Because the expander is limited to 1.5 dB steps, the compressor must be too. So the input power detector must generate the companding gain level signal in 1.5 dB steps also.

The placement of the compressor and the expander should reduce the noise caused by both the $\Delta\Sigma$ modulator and the DCT. This is additionally beneficial because the $\Delta\Sigma$ quantization noise, which occurs for small values of F_s and OSR, is now expected

to reduce also. The receiver path with the addition of companding should increase the SNR for small input power levels, especially when the Rx path is operating at a less calculation intensive base (low F_s and OSR).

Though not simulated as such, the compressor can also be moved before the ZOH to conserve power consumption as shown in Figure 4-2.

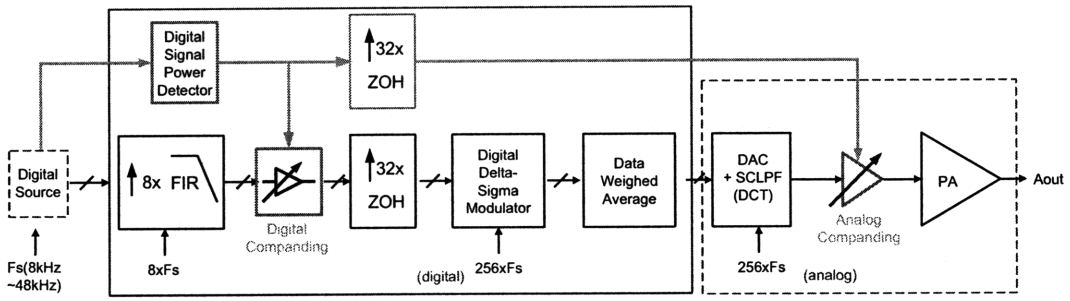

Figure 4-2: An alternative audio receiver path with companding. The compressor in this system is moved in front of the ZOH in order to preserve power consumption.

Chapter 5

Syllabic companding and transients

With syllabic companding, transients are formed at the output whenever a change in signal power level is detected. The $\Delta\Sigma$ modulator and the DCT, the modules between the compressor and expander, are filters with memory. A change in the signal power level causes the companding gain level to change. But the $\Delta\Sigma$ modulator and the DCT cannot process the change instantaneously, due to the delays in both the forward paths and the feedback paths of the filters, causing transients to occur. A single delay in the forward path is easy to compensate for by simply adding a delay to the attenuation or expansion block. In the case of an FIR (Finite Impulse Response) filter, the average delay can be applied to the expander in order to mitigate the transient effects of companding. However, delays in the feedback path, such as those in IIR (Infinite Impulse Response) filters, are much harder to eliminate.

5.1 A simple example

Take a look at a simple first order IIR filter, represented by a difference equation in Equation 5.1. The signal x is the input and y is the output.

$$y[n] = x[n] - \alpha(y[n-1]) \tag{5.1}$$

Companding is implemented by adding a compressor before the feedback loop

and an expander after the feedback loop. The system of equations for the newly companded system is represented in Equation 5.2a, Equation 5.2b, Equation 5.2c and Equation 5.2d. The function $g[n]$ represents the companding gain level signal provided by power detector.

$$x_*[n] = g[n]x[n] \tag{5.2a}$$

$$y_*[n] = x_*[n] - \alpha(y_*[n-1]) \tag{5.2b}$$

$$y[n] = \frac{y_*[n]}{g[n]} \tag{5.2c}$$

$$y[n]g[n] = x[n]g[n] - \alpha(y[n-1]g[n-1]) \tag{5.2d}$$

If $g[n]$ is held constant at a value g_1, then the system equation becomes Equation 5.3, which can reduce to the original filter in Equation 5.1.

$$y[n]g_1 = x[n]g_1 - \alpha(y[n-1]g_1) \tag{5.3}$$

If $g[n]$ is dynamic, the companding system can no longer reduce to the original filter. Assume $g[n]$ is modeled as a step function, taking on the value g_1 for a given amount of time, then transitioning to g_2 at time $n = k$. The function is modeled in Equation 5.4.

$$g[n] = \begin{cases} g_1, & \text{if } n < k \\ g_2, & \text{if } n \geq k \end{cases} \tag{5.4}$$

At $n = k$, $g[n]$ changes from g_1 to g_2 and the system equation becomes Equation 5.5, which cannot be reduced to Equation 5.1, the original system equation. While the effects of the error diminishes at α^2, no additional error is generated at, $n = k + 1$, as g[n] becomes constant again. However, a transient is now formed as a result of the delay in the feedback path.

$$y[k]g_2 = x[k]g_2 - \alpha(y[k-1]g_1) \tag{5.5}$$

Like the first order filter example, the $\Delta\Sigma$ modulator and the DCT behaves similarly because the two combined act as a 3^{rd} order IIR filter. Syllabic companding causes transients in the receiver path because the system is not memoryless.

5.2 Frequency domain analysis

The transient can also be explained through frequency domain analysis. Like any system, the $\Delta\Sigma$ modulator and the DCT can change the phase of the signal, causing delays at their output. However, the companding gain level signal is sent to the compressor and the expander simultaneously. The mismatch between the input and the output of the $\Delta\Sigma$ modulator and the DCT is a cause for the transient.

Furthermore, the spectrum of the compressed signal, the input signal multiplied by the companding gain signal, is no longer an inband signal due to the discontinuities caused by the step functions. In the original system, the frequency spectrum of the input is limited to the inband and the input is processed such that the inband signal is maintained while the outband noise is reduced. For this reason, the phase of the outband signal is considered inconsequential and the system was designed to be linear-phase inband only. However, when companding is added to the system, the spectrum of the compressed signal is actually spread across all frequencies. Thus, the $\Delta\Sigma$ modulator and the DCT no longer act as linear-phase filter at points of gain level transitions, causing the appearance of transients.

5.3 Transient compensation methods

Various methods exist to compensate the transients introduced by companding, [13] and [11]. The most basic form of compensation is simply applying a delay to the attenuator in the companding system and is one of the methods described in this section.

Additionally, a commonly used form of compensation is described in detail in Appendix Section A.1 and was discussed by Tsividis in [13]. To briefly summarize, the

coefficients within the signal processor are dynamically changed to follow concurrent changes in the companding gain signal. The coefficients are replaced such that there is no memory of the previous gain level in the filter state variables. Many companding systems choose this technique because it is easy to implement. Some examples are a translinear filter, a fifth-order Chebychev low-pass filter, a ADC as a part of a low-power hearing aid, and an audio reverberator, see [4], [7], [9], and [5] respectively. In all the examples, the predicted SNR was reached without being affected by transients.

In the CODEC audio receiver case, however, the state variable correction method is not implemented because of the presence of the nonlinear second order $\Delta\Sigma$ modulator. To change the coefficients of the modulator may result in unstable operating points. Thus a design decision was made to leave the $\Delta\Sigma$ modulator as is and to look for other methods of compensation.

Two additional methods are presented in [11]. Given as alternatives to state variable correction, they are the zero-crossing method, which is the second method described in this section, and the add-compensation method which is described in Appendix Section A.2. They are termed as non-invasive because they do not require changing the signal processor. However, both methods require the companding gain signal to be a series of step functions: compensation is required only at the step changes in the gain signal. This requirement puts a huge limitation on the types of companding systems for which the compensation methods can be used. While [11] gives examples of two types of companding systems, a second-order band-pass filter and a second order biquad filter, there have not been many, if any, actual implementation of the two compensation method recorded.

Luckily, the theory behind the two methods discussed in [11] may work well for the audio CODEC receiver since the companding gain signal is limited to 1.5 dB steps and compensation for the transients can be performed without modifying the $\Delta\Sigma$ modulator. After further inspection, the zero-crossing method was chosen instead of the add-compensation method because the add-compensation method would have required an addition module in either the 4-bit $\Delta\Sigma$ domain or the analog domain. Addition at either location is impractical and the method was abandoned for the

purpose of this thesis.

5.3.1 Filter gain signal compensation

As discussed above, the original companding system, see Figure 4-1, sends the gain level signal to both the compressor and the expander simultaneously while the $\Delta\Sigma$ modulator and the DCT, due to their phase characteristics, cause delays in the signal. Thus transients occur at sudden changes in the companding gain level because the system cannot instantaneously process these changes.

The first compensation method reduces the transient by delaying the companding gain signal that controls the expander. The method adds an additional filter that has the same frequency response as the Delta Sigma modulator and the DCT but with its gain normalized. The filter is a third order IIR low-pass filter. Because the DCT has a variable cutoff frequency which depends on the OSR of the system, the frequency response of the new filter will also be variable. However, the power amplifier, or the expander, limits the companding gain level signal to be in 1.5 dB steps. A threshold is then applied to the output of the additional filter; so the filter acts as a variable delay block to the companding gain signal. The block diagram of this system is shown in Figure 5-1.

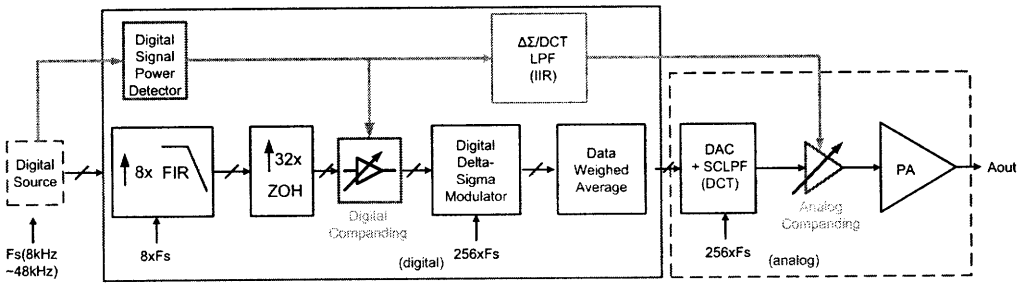

Figure 5-1: The companding gain signal that controls the expander is filtered by a normalized LPF with the same frequency response as the $\Delta\Sigma$ modulator and the DCT. The additional filter creates a delay in the gain signal that mimics the delay caused by the $\Delta\Sigma$ modulator and the DCT in the signal path.

Like the original companding system, the compressor in this system can be moved in front of the zero order hold to reduce power conservation. This system is shown in

Figure 5-2.

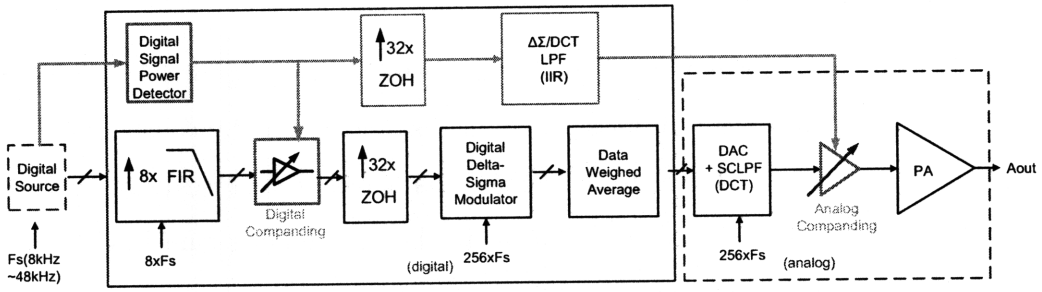

Figure 5-2: The compressor can be moved in front of the ZOH to reduce the number of multiplications required. This results in a less power consumptive system.

This filter compensation method can only minimize the delay mismatching that occurs between the compressor and the expander. It cannot reduce the transients that occur as a result of the feedback paths within the $\Delta\Sigma$ modulator. For this reason, a second compensation technique was studied.

5.3.2 Zero-crossings compensation

The transient caused by syllabic companding can also be reduced if the timing of the companding gain signal changes can be controlled. The second compensation method looks for the zero-crossings of the state variables within the system and changes the gain level signal only at the zero-crossings.

Equation 5.5 from Section 5.1 is reproduced below as Equation 5.6a. Recall that this system equation describes a first order filter with companding. At $n = k$, the companding system cannot replicate the original filter. The state variable in this first order filter is the output, $y[n]$. If the companding gain level signal changes to g_2 at the sample point when $y[k-1]$ is approximately zero, then Equation 5.6a can be reduced to Equation 5.6b, reducing the transient that occurs. This compensation method reduces the transients that that occur within the feedback path of the filter.

$$y[k]g_2 = x[k]g_2 - \alpha(y[k-1]g_1) \tag{5.6a}$$

$$y[k]g_2 \approx x[k]g_2 \tag{5.6b}$$

Figure 5-3 plots an example of the zero-crossing compensation system, but in continuous time. The top graph refers to the input power signal. The second graph, $x(t)$, represents the output of the companding system. The bottom graph, $A(t)$, is the companding gain signal generated by the zero-crossing logic. The first dash line indicates when the original gain level signal would have changed and when the zero-crossing logic turns on. The second dash line is the sample time when a zero has been detected at the output. At that time, $A(t)$ finally transitions to its new value.

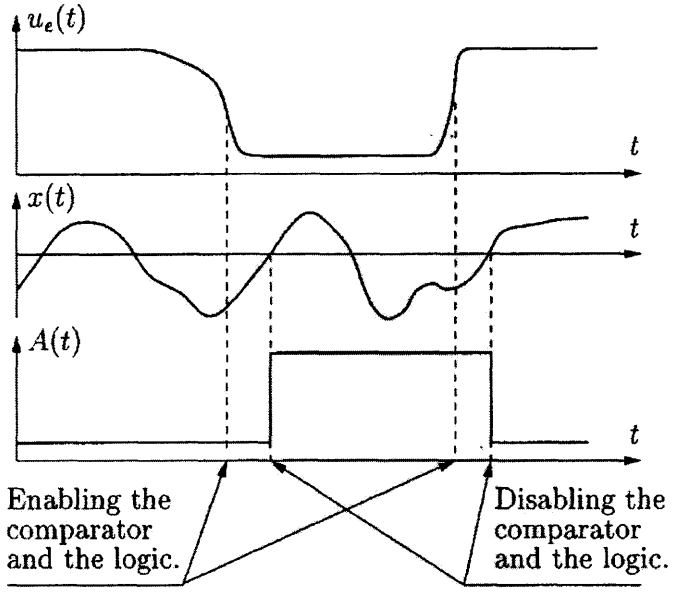

Figure 5-3: The zero-crossing logic is turned on when the gain level signal generated by the input power detector changes. The logic changes the new gain level signal when it detects a zero at the output of the DCT [11].

To implement the zero-crossing method, the gain level signal must be generated by the input power detector as a series of step functions. For the audio receiver path, this is not a setback because the expander, or the power amplifier, operates in 1.5 dB steps. In this second compensation system, there are two gain level signals: the signal generated by the detector and the signal generated by the zero-crossing logic. The majority of the time, the two gain level signals are equal. The zero-crossing logic is activated by a change in the original companding gain level. When activated, the

logic looks for a zero in the output of the DCT. When a zero is detected, a level change occurs in the the new signal gain level. The gain level signal generated by the zero-crossing logic controls the compressor and expander [11].

The block diagram of receiver path with companding and zero-cross compensation is shown in Figure 5-4. To simplify the detection at the output of the DCT, the analog DCT is replicated by a digital filter so that detection can be done in the digital domain. The digital DCT reflects its analog counterpart and is simply a first order IIR filter. While the new filter and the zero-crossing detector may be power intensive, they only need to be turned on when a change has occurred in the original companding gain level.

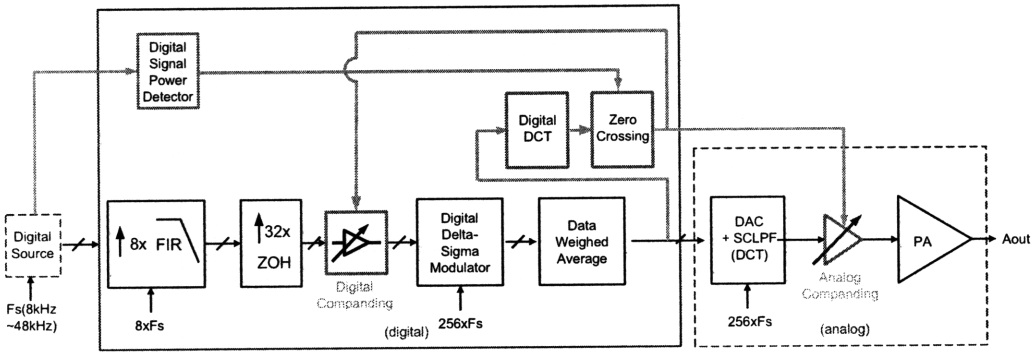

Figure 5-4: In this system, the gain level signal generated by the input power detector does not control the compressor and expander directly. Zero-crossing logic is added in the middle such that a change in the original gain level signal is delayed until a zero is detected at the output of the DCT.

In most cases, the zero-cross method becomes more complicated with higher order filters. A zero-crossing must be detected for each state [11]. For the CODEC receiver path, the zero-crossing method will only be applied to the DCT block, which is a first order filter. Because the signal processed by the $\Delta\Sigma$ modulator is operating at an oversample frequency, a zero should occur at the output of the DCT approximately around the same sample point as when a zero would appear in the states of the $\Delta\Sigma$ modulator. So detecting a zero at the output of the DCT should suffice.

Other compensation systems exist, but their implementation requirements extending beyond the design of the audio receiver path. Appendix A analyzes these other

techniques.

Chapter 6

Non-linear simulations: static companding

The newly designed CODEC receiver path with syllabic companding is first tested with constant companding gain levels to simulate static companding. Without any changes in the gain level signal, transients are not generated in the output of the system, allowing the simulations to verify that the dynamic range of the receiver path can be improved with companding. Because the companding gain signal in these simulations remains at constant, only one of the companding systems is simulated: the companding system without any compensation method; the compensation methods discussed in Chapter 5 only affect companding during changes in compression and expansion and will produce the same results in static companding.

6.1 Simulation setup

The simulations are conducted using a single-tone sinusoid input, coded into 16 bits. The frequency of the sine wave is set at 1020 Hz, which is defined by the A-weighting function as the most sensitive frequency to the human ear. The simulations test the effects of companding at various input amplitudes and companding gain levels. The input signal is tested with amplitudes of -20 dBFS, -40 dBFS, -60 dBFS, and -80 dBFS. In order to understand how the companding level will affect the signal to

noise ratio, the functionalities of the detector are not engaged. Instead, the system is fed with pre-determined gain signals at 1.5 dB, 4.5 dB, 9 dB, 15 dB, 19.5 dB, and 30 dB. Note that each of the companding gain levels is limited to 1.5 dB steps due to the limitations of the power amplifier.

To ensure comprehensiveness, other system variables are also simulated at various values. The input signal is sampled at the limits of the system, 8 KHz and 48 KHz. All three possible OSRs, 64x, 128x, and 256x, are fully tested. The analog noise in the DCT is simulated to be white Gaussian, with power strengths of -100 dBFS and -90 dBFS. All simulations are performed in Matlab. Simulation variables and their values are summarized in Table 6.1.

Table 6.1: The Simulation Parameters for non-linear, static companding are listed below.

Variable	**Used in simulation**
Sampling Frequency, F_s	8 KHz and 48 KHz
Input - number of bits	16
Over-sampling Ratio (OSR)	64x, 128x, 256x
Input Tone Frequency	1020 Hz
Input Amplitude, A	-20 dBFS, -40 dBFS, -60 dBFS, -80 dBFS
Gain Level, g	1.5 dB, 4.5 dB, 9 dB, 15 dB, 19.5 dB, 30 dB
Noise injected at DCT	-100 dBFS WGN, -90 dBFS WGN, no noise

6.2 Simulation results

The purpose of the static simulations is to understand the effects of companding at various companding gain levels. Other variables are changed for the sake of thoroughness in order to comprehend how companding affected the system at various settings. Analyzing the results of these tests, a number of trends emerges.

First and foremost, companding at every gain level results in an increase in the output SNR. At its best, companding improves the output SNR by 22.7 dB. These results show that companding is a viable method to improve the output SNR of the audio receiver path.

The SNR improvements vary exponentially according to the companding gain

level. In other words, the benefits of companding eventually reach an asymptotic limit. Using a companding gain level of 9.0 dB instead of 4.5 dB improves the output SNR more effectively than using a companding gain level of 30 dB instead of 19.5 dB. Figure 6-1 graphs the improvements in the output SNR as it approaches its maximum. The figure plots the simulation results at F_s = 8 KHz, OSR = 256x, and with a -90 dBFS noise injected at the DCT. Each line plots the SNR improvements for various input amplitudes as the companding gain level is set from 1.5 dB to 30 dB. The asymptotic approach indicates that a gain level of 20 dB will result in approximately the same SNR improvement as a gain level of 30 dB. Thus, the companding system's input power detector needs to generate a companding gain level of only 20 dB in order improve the SNR at the output of the audio path.

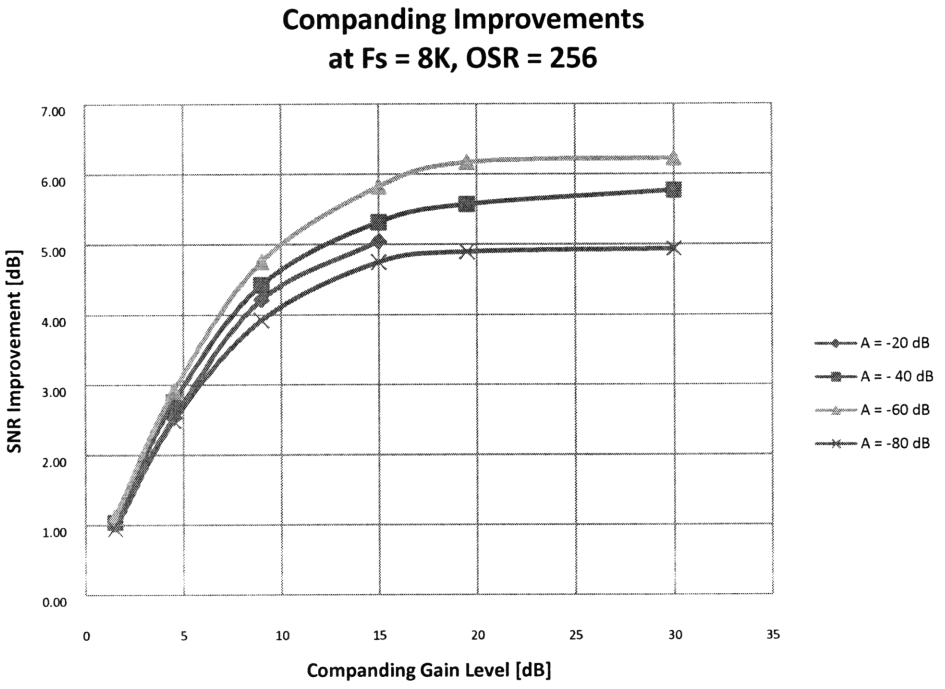

Figure 6-1: The graph analyzes the static results of applying companding to the receiver path. The SNR improvements at 8 KHz sampling frequency and 256x OSR are plotted. -90 dBFS noise is injected at the DCT. Each line represents the rise in SNR for different input amplitudes at various companding gain level. The figure shows that companding improves the SNR at the output exponentially as the gain level is increased.

As companding diminishes the effect of the noise sources within the receiver path, the input quantization noise becomes more important in the SNR measurements. The effect of the input quantization noise is apparent when comparing the output SNR for injecting -90 dBFS noise and -100 dBFS noise. At high sampling frequencies,the input quantization noise becomes the dominant noise source when injecting -100 dBFS WGN into the DCT. Since the output SNR is limited by the dominant noise, companding improvements are much lower with -100 dBFS DCT noise compared to -90 dBFS DCT noise. This is demonstrated in Figure 6-2 and Figure 6-3. At the higher sampling frequencies and OSRs, the SNR improvements with -100 dBFS DCT noise are more than 6 dB lower than that with -90 dBFS noise. Fortunately, the receiver path is designed such that the input to the receiver path can be encoded in up to 24-bits, so companding can still have a strong impact in the output SNR.

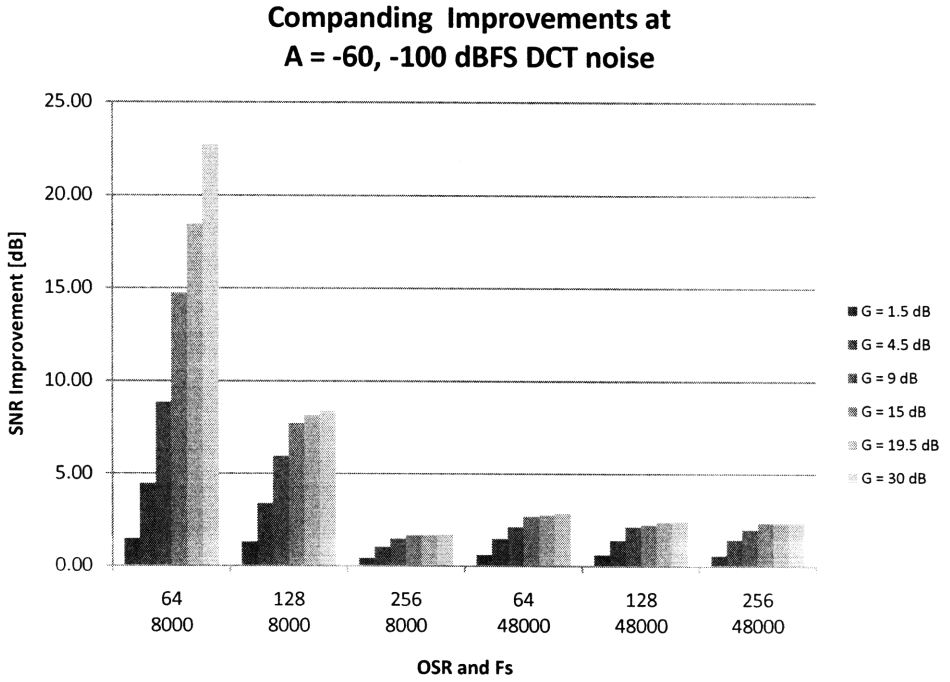

Figure 6-2: SNR improvements at the output of the receiver path are plotted. The SNR improvements are arranged according to the sampling frequency and OSR, and then by the companding gain level used.

The improvements made by the companding techniques can be summarized by

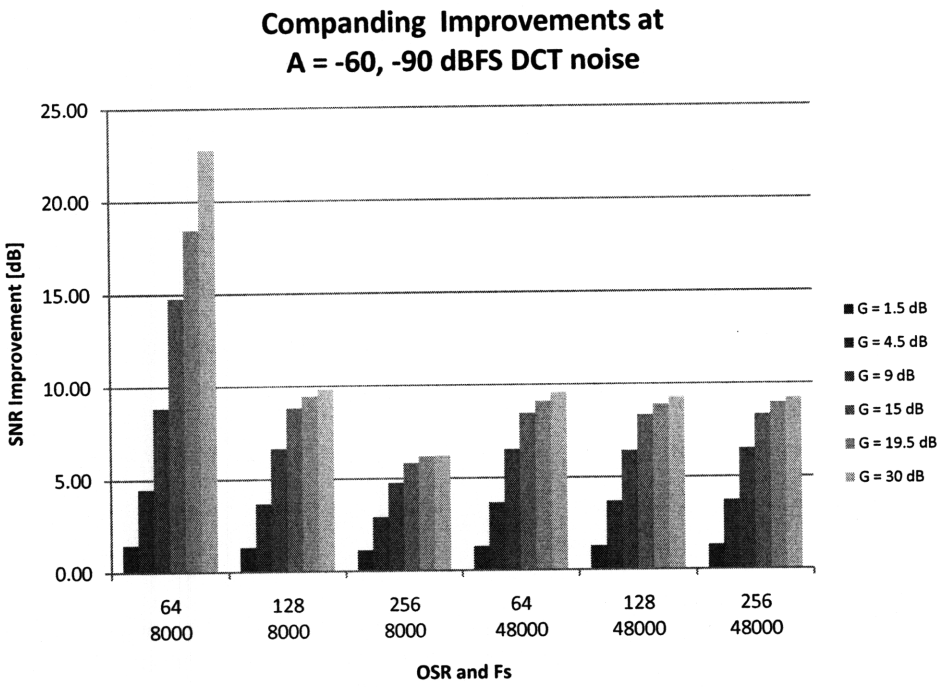

Figure 6-3: SNR improvements at the output of the receiver path are plotted. The SNR improvements are arranged according to the sampling frequency and OSR, and then by the companding gain level used.

calculating the dynamic range at the output. Dynamic range is calculated by the A-weighted output SNR + 60 dB when the input signal has an amplitude of -60 dBFS. Table 6.2 summarizes the dynamic range improvements of the system with both -90 dBFS and -100 dBFS DCT noise injection at various sampling frequencies and OSRs.

The table shows that companding with a 20 dB compression gain can increase the dynamic range of the audio CODEC receiver path by up to the 18.44 dB at the lowest sampling frequency and over-sampling ratio. At the highest F_s and OSR, the companding system can increase the dynamic range of the system by either 2.33 dB or 8.96 dB, depending on how much noise is injected at the DCT. These static simulations indicate that companding is a viable method to increase the dynamic range of the receiver path. The next chapter will simulate the companding system dynamically to explore the transients that incur.

Table 6.2: The dynamic range improvements were calculated from measuring the SNR at the output of the companding system. The improvements are listed for both -100 dBFS DCT noise and -90 dBFS DCT noise.

Fs	**OSR**	**Dynamic Range Improvements with -100 dBFS DCT noise**	**Dynamic Range Improvements with -90 dBFS DCT noise**
8 KHz	64 x	18.43 dB	18.44 dB
8 KHz	128 x	8.14 dB	9.46 dB
8 KHz	256 x	1.66 dB	6.17 dB
48 KHz	64 x	2.73 dB	9.12 dB
48 KHz	128 x	2.36 dB	8.91 dB
48 KHz	256 x	2.33 dB	8.96 dB

Chapter 7

Non-linear simulations: dynamic companding

The companding systems are now tested with a variable companding gain signal. The three systems listed in Chapter 5 are simulated in this section: syllabic companding without any compensation; syllabic companding with an additional filter to add a delay to the companding gain signal that controls the expander; and syllabic companding with zero-crossing method to control gain level changes. They are hereafter referred to as System 1, System 2, and System 3, respectively.

The transients are measured by comparing the outputs of each of the three companding systems with the output of the original system, referred to as System 0.

7.1 Simulation setup

Like in Chapter 6, the systems are tested with a single tone sinusoid input with tone frequency of 1020 Hz and sampled at 16-bits. Likewise, the minimum and maximum sampling frequencies, 8 KHz and 48 KHz are simulated with OSRs of 64x, 128x, and 256x. In these simulations, however, only one input amplitude is tested, at -41 dBFS.

Like the static simulations, the signal power detector block is not simulated. Instead, its behavior is modeled by a companding gain signal that is controlled by time constants, T_{attack} and T_{decay}. T_{attack} is the amount of time required for the compand-

ing gain signal to react to an increase in signal power; T_{decay} is the amount of time required for for the companding gain level to react to a decrease in signal power. In each simulation, two gain level are used, g_1 and g_2. The signal is held constant at an initial gain level, g_1, for the first half of each test. The gain level then transitions to the final gain level, g_2. Due to the limitations of the expander, the transition occurs in 1.5 dB steps according to either T_{attack} or T_{decay}. For the remainder of each simulation, the gain level signal is then held constant at g_2. Various gain levels between 0 dB and 20 dB are simulated for both g_1 and g_2. The values used for each test variable is listed in Table 7.1. Each permutation of parameters is simulated 50 times in Matlab, and the results are averaged and presented here.

Table 7.1: The Simulation parameters for non-linear, dynamic companding are listed below.

Variable	**Used in simulation**
Sampling Frequency, F_s	8 KHz and 48 KHz
Input - number of bits	16
Over-sampling Ratio (OSR)	64x, 128x, 256x
Input Tone Frequency	1020 Hz
Input Amplitude, A	-41 dBFS
T_{attack}	10 mS
T_{decay}	40 mS
Gain Level Pairs, (g_1, g_2)	(0, 19.5), (9, 19.5), (18, 19.5), (19.5, 18), (19.5, 9), (19.5, 0)
Noise injected at DCT	-100 dBFS WGN

A last parameter that has not been discussed is the expander attenuation error, which is inherent in the power amplifier. The PA can change the attenuation to the signal by up to ± 0.5 dB. The dynamic companding simulations are performed both with and without this error. To simulate the attenuation error, a randomly generated value from -0.5 dB to 0.5 dB is added to the attenuation factor at each unique value in the gain level signal. In other words, these simulations add an error to g_1, g_2, and at each 1.5 dB step during the transition from g_1 tp g_2.

An example of the gain level signals during a transition is shown in Figure 7-1. Figure 7-1(a) depicts a perfect transition from g_1 to g_2. Figure 7-1(b) is the same transition, but constrained to 1.5 dB steps. This signal is the gain level signal that is supplied to the compressor in System 1 and System 2. The gain signal supplied to the

expander in System 1, which may have a ± 0.5 dB error due to inaccuracies in the PA, is shown in Figure 7-1(c). At each level, the signal Figure 7-1(c) deviates by a small amount from that of Figure 7-1(b). The signal in Figure 7-1(d) is the companding gain level supplied to the expander in System 1, but filtered by the additional IIR in System 2. Because the expander is limited to 1.5 dB step, the IIR filter causes a minute delay in the signal. The last graph, Figure 7-1(e), depicts the gain level signal to be supplied to the expander in System 3. The delay in the transitions of Figure 7-1(e) is caused by the zero-crossing algorithm: the gain level remains constant until it detects a zero in the output. The gain level supplied to the compressor is that of Figure 7-1(e) but without the attenuation errors.

Without the ± 0.5 dB attenuation error, the transients can be measured accurately by simply subtracting the output of each companding system by the output of the original system, the reference signal. The result of the subtraction, which represents the noise and the transients at the output, is then A-weighted and the local maximums are found.

With the ± 0.5 dB error in attenuation, the noise and transient cannot be calculated from simply subtracting the companding outputs from the reference output. Instead, the noise and transient is calculated as in Figure 7-2. Since the attenuation error at every sample point is known by the simulation, the reference signal is first multiplied by the attenuation error so that the two output signals can be compared. When subtracting, the deltas that occurred from changes in the attenuation error are then added back into the comparison in order to ensure the measurement of all the transients. The noise plus transient is then processed by A-weighting. At each 1.5 dB step, the transient is measured by the local maximum.

7.2 Example output

Example noise plus transient outputs for each system is shown in Figure 7-3. These simulations are done at $F_s = 48$ KHz and OSR = 64. The initial gain is set at 9 dB; final gain is set at 19.5 dB. In each figure, top graph plots the A-weighted noise plus

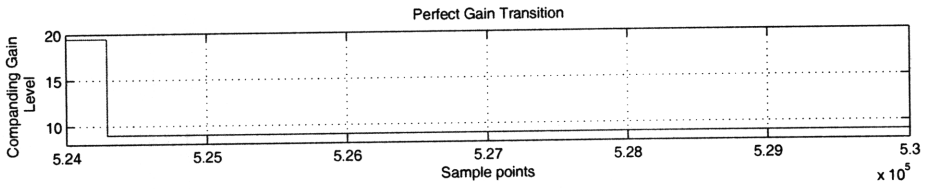

(a)

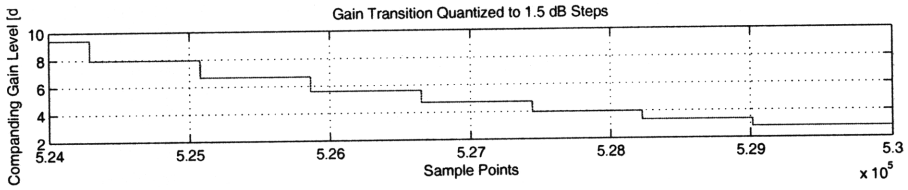

(b)

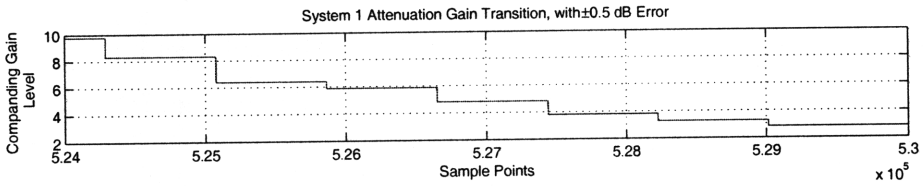

(c)

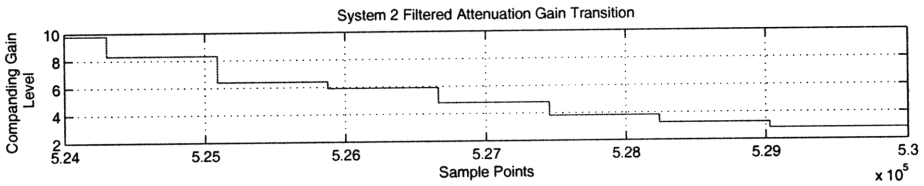

(d)

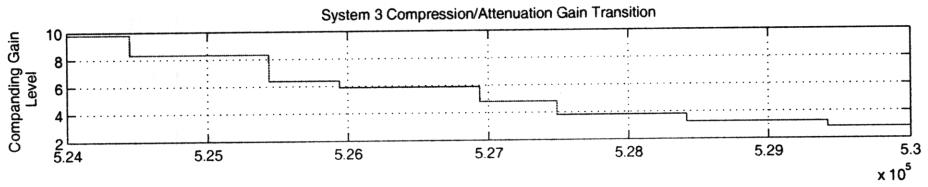

(e)

Figure 7-1: An example of the the companding gain level transitions for the various companding systems is shown.

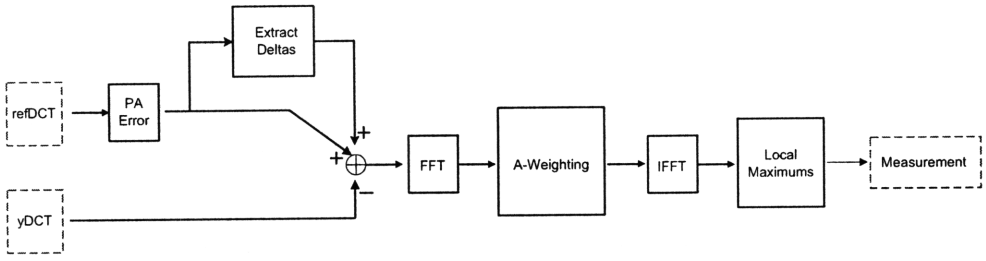

Figure 7-2: With the presence of ±0.5 dB attenuation noise, the transients are measured according to the block diagram in the figure.

transient at the output of the DCT. The bottom three graphs starting from the left are the variance of the noise plus transient at the initial gain level, the transition, and the final gain level. The middle graph is overlayed with the companding gain level signal.

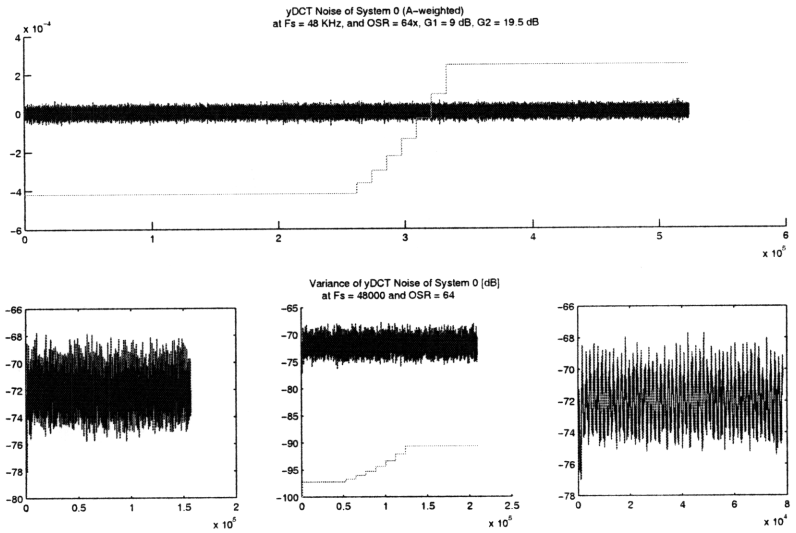

(a) Original audio Rx path

Figure 7-3: The top graph is a plot of the noise and transient [V] at the output of the DCT. The bottom three graphs are the variance of the noise plus transient at the output at the the initial g_1, the transition period, and the final g_2.

Figure 7-3 shows that transients occur when using each of the companding systems. These transients happen at the transitions of the companding gain level signal. However, the transient peaks in System 2 and System 3, are much smaller than that of System 1, indicating that the compensation methods of this thesis is performing

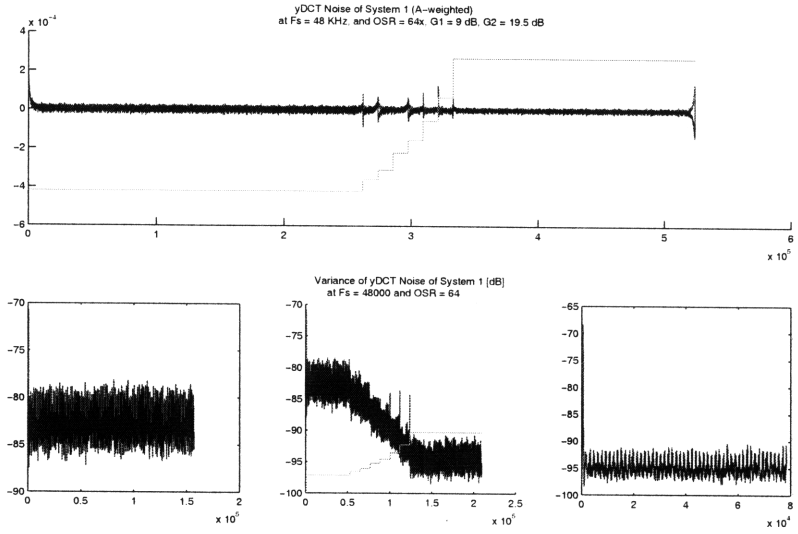

(b) Companding system without any compensation

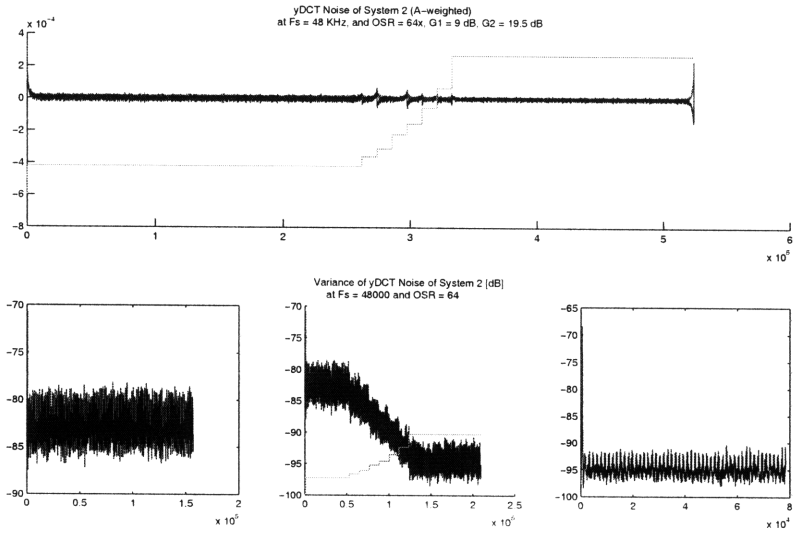

(c) Companding system with filtered attenuation gain signal

Figure 7-3: The top graph is a plot of the noise and transient [V] at the output of the DCT. The bottom three graphs are the variance of the noise plus transient at the output at the the initial g_1, the transition period, and the final g_2. (cont.)

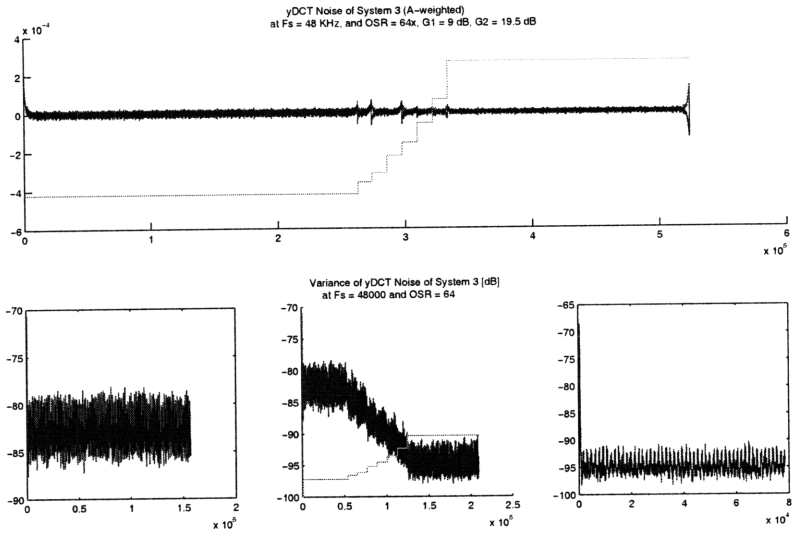

(d) Companding system with zero-crossing detection

Figure 7-3: The top graph is a plot of the noise and transient [V] at the output of the DCT. The bottom three graphs are the variance of the noise plus transient at the output at the the initial g_1, the transition period, and the final g_2. (cont.)

well.

7.3 Simulation results

The results of the dynamic simulations are presented in this section. In all the simulations, the transients formed in System 2 and System 3 are consistently lower than the transients formed in System 1, demonstrating that the compensation methods discussed in Chapter 5 are valid for the audio Rx path. Figure 7-4 plots the relative peak amplitude for each companding systems with various pairings of (g_1, g_2) for F_s = 8 KHz, OSR = 256x in Figure 7-4(a), and F_s = 48 KHz, OSR = 128 KHz in Figure 7-4(b).

The graphs plot the relative transients peaks of each system at different (g_1, g_2) configurations. The relative transients peaks are calculated as the difference between the maximum peaks in the transients of the companding systems and the maximum noise level of the original audio receiver path. When the companding gain level is

constant, at the beginning and the end of each simulation, there are no transients and all the systems act identically. The differences calculated are equal for the three systems and simply represent the difference in the noise levels for static companding; these values are plotted in black in Figure 7-4. The relative transients peaks of each companding system during the gain level transition periods are plotted in gray.

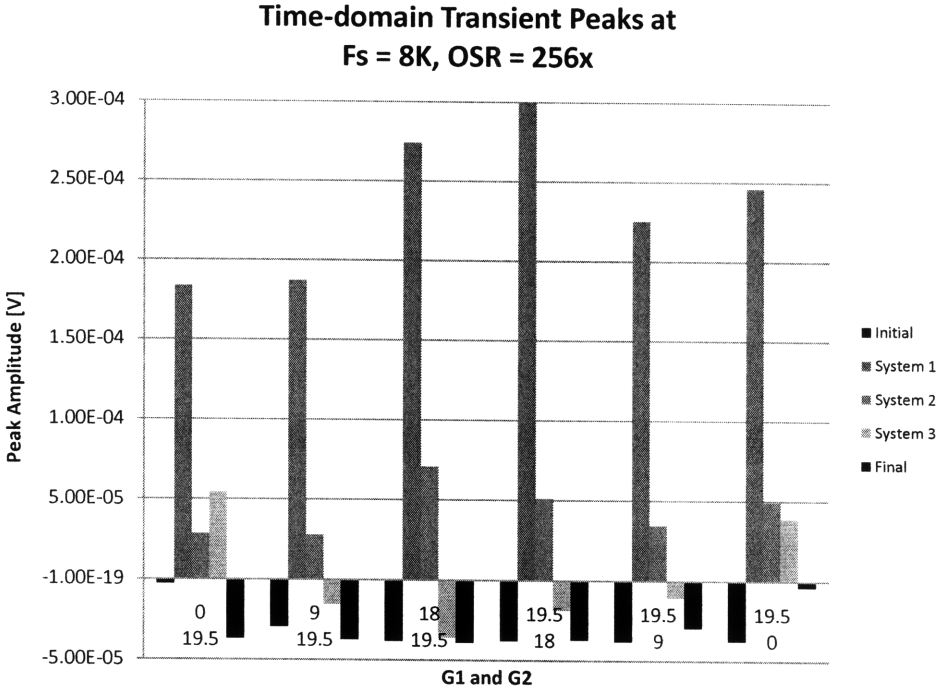

(a) F_s = 8 KHz, OSR = 256x

Figure 7-4: The relative transient peaks of the three companding systems are plotted in the graph. Each group of five bars shows the simulation result for a specific (g_1, g_2) pairing. The black bars in the beginning and the end of each group plot the static noise difference between the companding system and the original system at g_1 and g_2. The gray bars in the middle compare the relative transient peaks for each companding system during the transition from g_1 to g_2.

In both Figure 7-4(a) and Figure 7-4(b), the transients are much lower in System 2 and System 3 than in System 1. The relative transient peaks calculated for System 2 and System 3 are about the same for when the results from all the (g_1, g_2) pairings are put together. However, for both figures, the transient peaks formed by System 3 are significantly higher when the change in the gain level signal is big, for example,

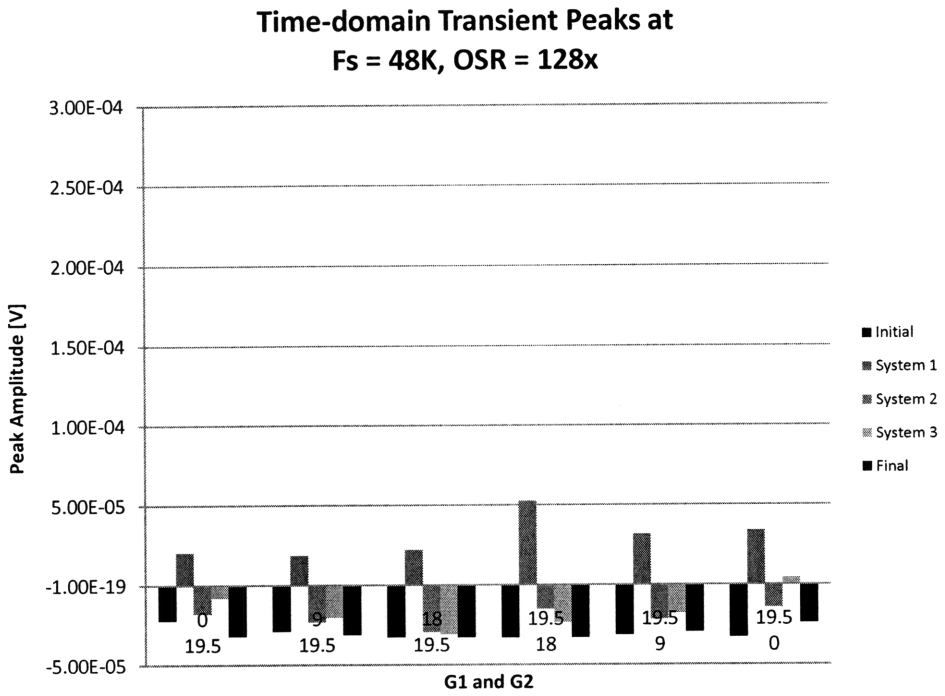

(b) F_s = 48 KHz, OSR = 128x

Figure 7-4: The relative transient peaks of the three companding systems are plotted in the graph. Each group of five bars shows the simulation result for a specific (g_1, g_2) pairing. The black bars in the beginning and the end of each group plot the static noise difference between the companding system and the original system at g_1 and g_2. The gray bars in the middle compare the relative transient peaks for each companding system during the transition from g_1 to g_2 (cont.).

at an initial gain level of 19.5 dB and final gain level of 0 dB or at an initial gain level of 0 dB and final gain level of 19.5 dB.

Further analysis indicated that the zero-crossing algorithm fails to detect a zero crossing at the output of the DCT when gain level is low. The quantization noise added during $\Delta\Sigma$ modulation can potentially create false zeros in the signal. In Figure 7-5, the top graph plots the noise plus transients during the companding gain level transition; the bottom graph plots the output of the DCT. Both graphs also plot the companding gain level signal. The data is taken from a single simulation run at F_s = 8 KHz, OSR = 128x, and (g_1, g_2) = (19.5 dB, 0 dB).

The algorithm behaves correctly in the beginning; the gain level signal transition

at zero crossings of the DCT output. As the companding gain level decreases, the noise in the output of the DCT with respect to the signal increases and real zero crossings are much harder to detect. The vertical dashed lines highlight two examples when the companding gain signal steps down without a zero crossing in the signal. Correspondingly, the transients that occur when the zero is falsely detected are significantly higher than the other transients.

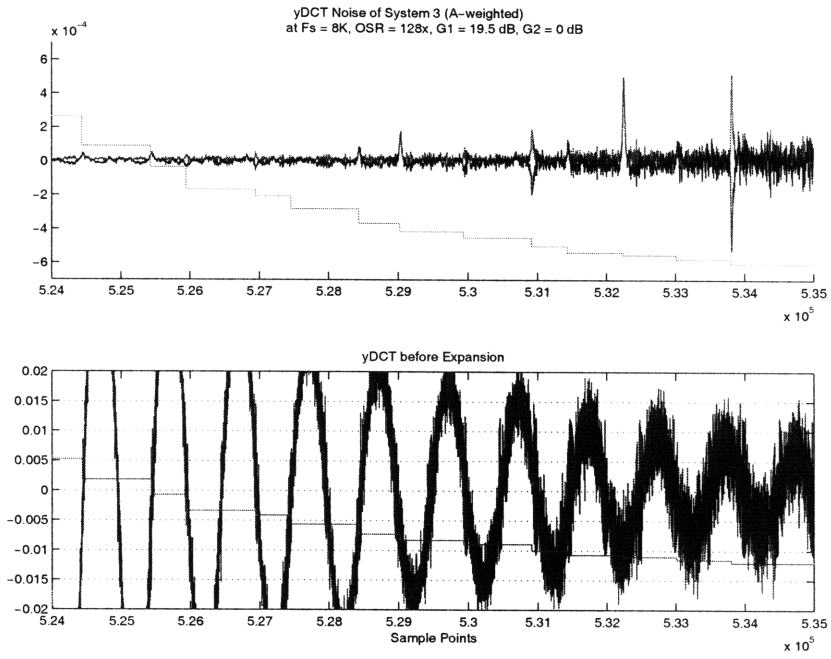

Figure 7-5: The effectiveness of the zero-crossing algorithm is analyzed. The top graph plots the noise plus transients during the companding gain level transition. Both the original signal and its absolute value is plotted. The bottom graph blots the output of the DCT. On top of each graph is the companding gain level signal. The vertical dashed lines indicates locations in time when the zero-crossing algorithm failed to correctly identify a zero in the output signal.

In real operation, the receiver path does not operate at the points where zeros are falsely detected in the output of the DCT. In the simulations, the input amplitude is kept constant while the companding gain level signal are raised and lowered causing the noise to increase relative to the signal strength. In real operation, the companding gain signal is decreased only if the amplitude of the input signal increases such that a high signal to noise ratio would be maintained throughout operation. This indicates

that the transients caused by the zero-crossing compensation method would be smaller in real operation.

Another trend in the transients formed by the three companding systems is shown in Figure 7-6. The figure compares the relative transient peaks across the different sampling frequencies and OSRs simulated when g_1 is set to 19.5 dB and g_2 is set to 9 dB. The relative transient peaks are grouped according to the sampling frequencies and OSR. It can be seen that at a lower F_s and OSR, the transients are significantly less noticeable because of the high SNR improvement resulting from companding. For example, since companding dramatically improves the SNR when $F_s = 8$ KHz, OSR $= 64$, the transients are no longer as visible as at higher sampling frequencies and OSRs.

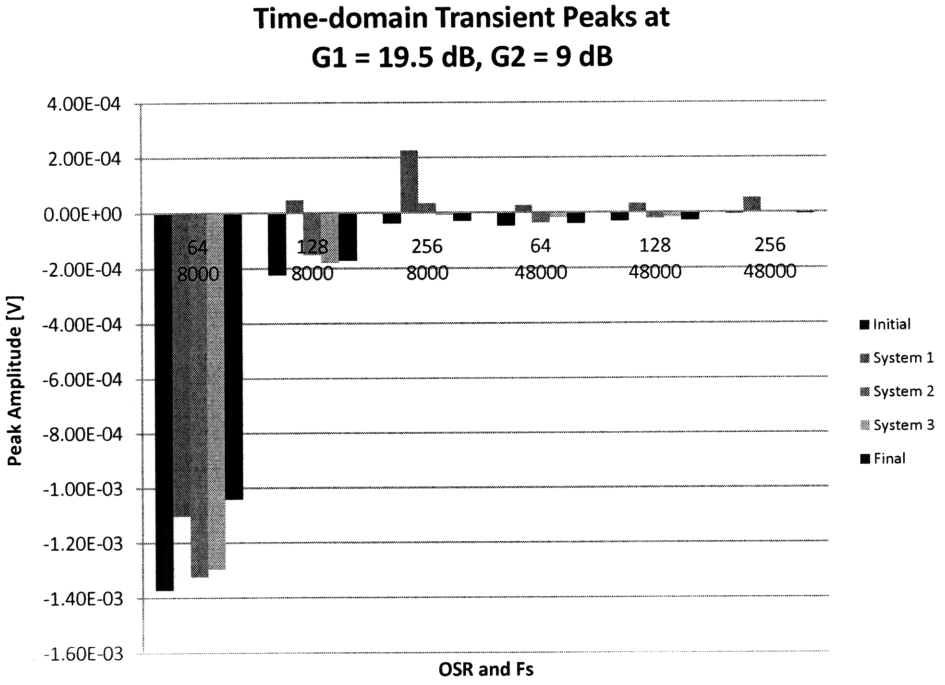

Figure 7-6: The relative transient peaks of the three companding systems are plotted. Each group of five bars shows the simulation result for a specific sampling frequency and OSR. The black bars in the beginning and the end of each group plot the static noise difference between the companding system and the original system. The gray bars in the middle compare the relative transient peaks for each companding system during the transition from g_1 to g_2.

The previous graphs have plotted the simulation results without an attenuation

error of up to ±0.5 dB error. Comparing the transient peaks with and without the addition of 0.5 dB shows that the relative transient peaks are almost the same, see Figure 7-7.

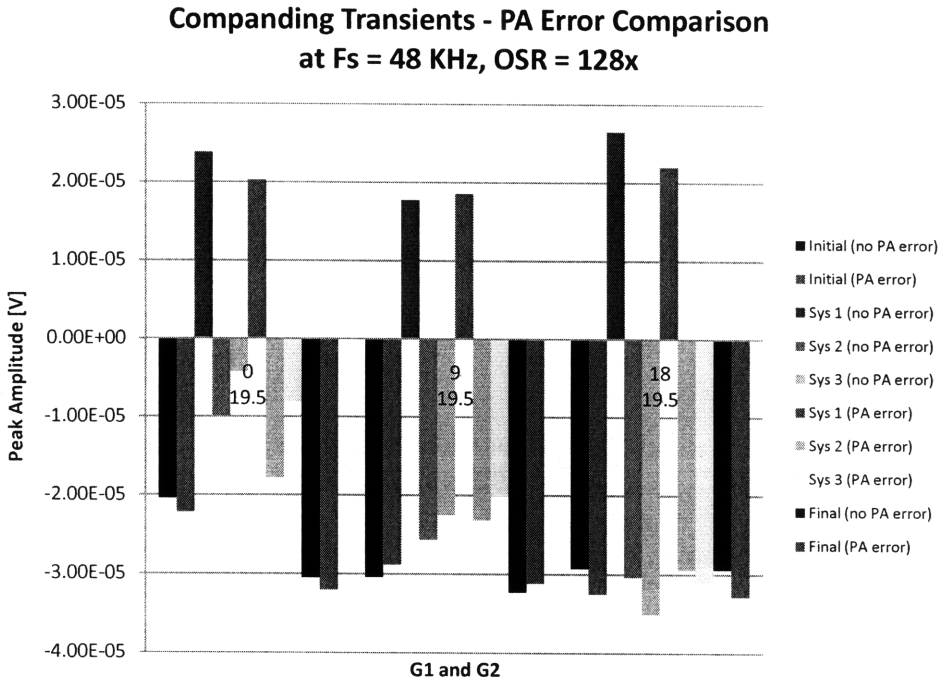

Figure 7-7: The relative transient peaks with and without ±0.5 attenuation error with three different (g_1, g_2) pairings. For each grouping, the two bars in the beginning and the end plot noise improvements of the companding the systems. The six bars in the middle plot the relative transient peaks for Systems 1, 2, and 3 without and with the attenuation error.

To summarize, the results of the dynamic simulations demonstrate that transients occur in the output of the audio receiver path when the companding gain signal transitions. Further, the compensation techniques described in Chapter 5 are able to reduce the amplitude of the transients.

The average peak amplitudes of the transients are given in Table 7.2 and Table 7.3. The amplitudes were averaged according to the initial and final gain level for compression. Averaging over all initial and final gain levels, System 2 and System 3 are able to reduce the transients of System 1 by 61%. Comparing System 2 and System 3 against each other, the table shows that System 2 performed better when

the initial or final companding gain level is low. However, in other situations, System 3 is better at reducing transients than System 2. This is consistent with the analysis, which concluded that the zero-crossing algorithm in simulation cannot always accurately detect a zero-crossing due to the high frequency noise generated by the $\Delta\Sigma$ modulator. However, the false readings only occur when the signal to noise ratio before the expander decreases, which is less likely outside of simulations because companding keeps the signal to noise ratio constant within the signal process. So transient results for real usage will most likely improve with System 3. Given that the average performance of System 2 and System 3 in simulation show that the two systems are equally capable of reducing transients, it can be assumed that System 3 is the better candidate to compensate for the transients that are caused by the companding system.

Table 7.2: The results of the dynamic simulations are averaged according to the initial and final companding gain signal. The data represents the actual amplitude and is measured in Volts.

		Average Peak Amplitude		
Initial Gain	**Final Gain**	**System 1**	**System 2**	**System 3**
0 dB	19.5 dB	1.87×10^{-5}	9.37×10^{-5}	1.29×10^{-4}
9 dB	19.5 dB	1.76×10^{-5}	6.71×10^{-5}	6.65×10^{-5}
18 dB	19.5 dB	2.21×10^{-5}	8.34×10^{-5}	3.52×10^{-5}
19.5 dB	18 dB	2.57×10^{-5}	7.68×10^{-5}	4.25×10^{-5}
19.5 dB	9 dB	2.11×10^{-5}	8.07×10^{-5}	7.68×10^{-5}
19.5 dB	0 dB	2.38×10^{-4}	1.14×10^{-4}	1.42×10^{-4}
Average		2.15×10^{-5}	8.59×10^{-5}	8.20×10^{-5}

Table 7.3: The results of the dynamic simulations are averaged according to the initial and final companding gain signal. The data shows how much the transients in System 2 and System 3 have been reduced as compared to System 1.

		% Decrease	
Initial Gain	**Final Gain**	**System 2**	**System 3**
0 dB	19.5 dB	49.90%	31.12%
9 dB	19.5 dB	61.89%	62.23%
18 dB	19.5 dB	62.31%	84.07%
19.5 dB	18 dB	70.15%	83.48%
19.5 dB	9 dB	61.77%	63.55%
19.5 dB	0 dB	52.02%	40.12%
Average		60.03%	61.84%

Chapter 8

Conclusion

The goal of the thesis is to improve the SNR of the audio CODEC Rx path for small input signals. Companding techniques are the focus of this project because they do not require a significant increase in power supply but still have the ability to reduce the effects of the $\Delta\Sigma$ quantization noise and the DCT analog noise.

In the simulations, it is shown that companding increases the dynamic range of the system by improving the SNR at the output of Rx path. However, transitions in the companding gain level signal causes transients to occur. The size of these transients can be reduced by compensation methods, as shown in Chapter 7.

8.1 Recommendations

Further improvements can be made on the audio receiver path with companding.

In addition, a power detector still needs to be designed to generate the companding gain level signal. The static companding results show that it is unnecessary for the detector to generate a companding gain level above 20 dB. To eliminate the possibility of saturation in the $\Delta\Sigma$ modulator, the detector should not generate a high gain signal when the input amplitude is high. It is recommended that the companding techniques are used only when the input power is below -20 dBFS. To reduce the occurrence of saturation, the companding gain should be generated such that a compressed signal's power is also limited to -20 dBFS. Above -20 dBFS, companding will not be utilized

and the companding gain level should be set at 0 dB. Figure 8-1 plots the input output curve of the input signal and the compressed signal.

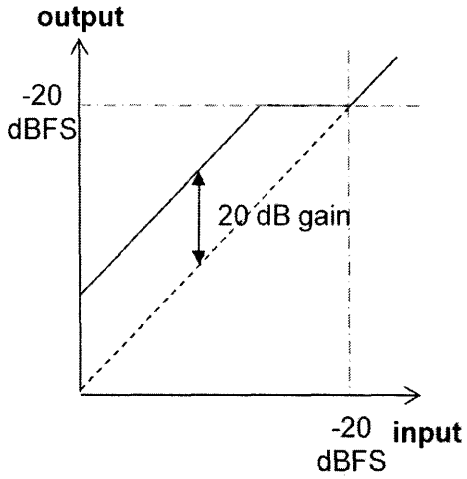

Figure 8-1: The input-output curve of compression, controlled by the detector, is shown. When the input signal is above -20 dBFS, the companding gain signal is set to 0 dB and there is a 1-1 matching between the input signal and the compressed signal. Below -20 dBFS, the input signal is compressed, or amplified, such that there is at most a 20 dB gain but limiting the maximum power of the compressed signal to -20 dBFS.

Analysis on the two compensation methods shows that at times the zero-cross module cannot accurately detect a zero crossing at the output of the DCT. When there is high $\Delta\Sigma$ quantization noise, false detections occur. While the occurrence of the misreading may be low, possibly insignificant, during actual operation, the false detections must be studied further. It may be possible to detect the zero crossings before the $\Delta\Sigma$ modulator if the delay that occurs is accurately accounted for. Detection before the $\Delta\Sigma$ modulator is more accurate because less high frequency noise is present at the modulator's input.

Appendix A

Other compensation methods

Two other transient compensation methods are discussed here. Because of the difficulties in implementation, the following methods are not included in the simulations.

A.1 System coefficient correction

Transients are formed in a companding system because a change in the companding gain signal is not automatically reflected in the state variables within the system. This effect was given in Equation 5.5 and reproduced in Equation A.1. Equation A.1 is the difference equation at $n = k$, when $g[n]$ transitions from g_1 to g_2.

$$y[k]g_2 = x[k]g_2 - \alpha(y[k-1]g_1) \tag{A.1}$$

The problem lies in the feedback path. Even though both $y[k]$ and $x[k]$ have the correct gain level, g_2, $y[k-1]$ is preceded by the gain level g_1. The problem can be solved by dynamically changing the value of α at time $n = k$. If at the transition from $g1$ to $g2$, α is changed to α_* as in Equation A.2, then the system difference equation at the transition point can be reduced to Equation A.6, eliminating the transients [13].

$$\alpha_* = \alpha\frac{g_2}{g_1} \tag{A.2}$$

$$y[k]g_2 = x[k]g_2 - \alpha_*(y[k-1]g_1) \tag{A.3}$$

$$y[k]g_2 = x[k]g_2 - \alpha\frac{g_2}{g_1}(y[k-1]g_1) \tag{A.4}$$

$$y[k]g_2 = x[k]g_2 - \alpha(y[k-1]g_2) \tag{A.5}$$

$$y[k] = x[k] - \alpha y[n] \tag{A.6}$$

While efficient and easy to implement in a digital processor, this compensation method is not chosen for the audio receiver path. The filter in the CODEC receiver path is the $\Delta\Sigma$ modulator and the DCT. A design decision was made given that the $\Delta\Sigma$ modulator is a non-linear feedback loop, dynamically changing the coefficients in the modulator may lead to operating the $\Delta\Sigma$ modulator at unstable points and ultimately break the system.

A.2 Feed-forward add compensation

Another compensation method is the feed-forward add compensation technique. A corrective signal, $c[n]$, can be added to the signal path to compensate for the transient caused at companding gain level transition. To find $c[n]$, let $y[n]$, the output of the companding filter system, be defined as in Equation A.7. The input, $x[n]$, is first compressed by multiplying by $g[n]$, convolved with the filter, $h[n]$, and expanded by dividing by $g[n]$.

$$y[n] = \frac{1}{g[n]}((g[n]x[n]) * h[n]) \tag{A.7}$$

Then the corrective signal, $c[n]$ can be calculated as shown in Equation A.9 where $h[n] * x[n]$ is the output of the original system without companding and $y[n]$ is the output of the system with companding.

$$c[n] = h[n] * x[n] - y[n] \tag{A.8}$$

$$= \frac{1}{g[n]}(g[n](h[n] * x[n]) - h[n] * (g[n]x[n])) \tag{A.9}$$

If we assume that g[n] is a step function, like in Equation 5.4, the companding gain signal can be also represented by Equation A.10 where the gain level changes from g_0 to g_1 at k and $U[n]$ is the universal step function.

$$g[n] = g_1 - (g_1 - g_0)U[k - n] \tag{A.10}$$

When $n < k$, $g[n]$ is constant, $y[n]$ equals $h[n] * x[n]$, and $c[n] = 0$. When $n \geq k$, $g[n]$ is replaced by Equation A.10, and $c[n]$ is calculated to be Equation A.12.

$$c[n] = \frac{1}{g_1}(g_1(h[n] * x[n]) - h[n] * (g_1x[n] - (g_1 - g_0)U[k - n]x[n])) \tag{A.11}$$

$$= \frac{g_1 - g_0}{g_1}h[n] * (U[k - n]x[n]) \tag{A.12}$$

To summarize, the corrective signal, $c[n]$ is defined as Equation A.13. To generate $c[n]$, a new filter and two switches are needed. The filter replicates the original filter, $h[n]$, with an additional gain $= \frac{g_1 - g_0}{g_1 g_0}$.

$$c[n] = \begin{cases} 0, & \text{if } n < k \\ \frac{g_1 - g_0}{g_1 g_0}h[n] * ((g_0x[n])U[k - n]), & \text{if } n \geq k \end{cases} \tag{A.13}$$

Figure A-1 is the block diagram of an implementation of a companding system with feed-forward compensation in continuous time. $A(t)$ represents the companding gain signal, $g[n]$, and transitions at $t = \tau$. When the companding gain level signal is constant, S_1 is set to the compressed input, $g_0x(t)$. At $t = \tau$, $A(t)$ changes to g_1, and S_1 flips to 0, or ground, to generate the signal $(g_0x(t))U(t - \tau)$ and feeds it to the input of the auxiliary filter. The second switch, S_2, is set to 0, or ground, when

$A(t)$ is constant. When a transition is detected, S_2 flips to the output of the auxiliary filter plus a gain block. Eventually, $c(t)$ decays to zero, S_2 is set back to 0 [11]. The block $G(t)$ is the gain factor, $\frac{g_1 - g_0}{g_1 g_0}$.

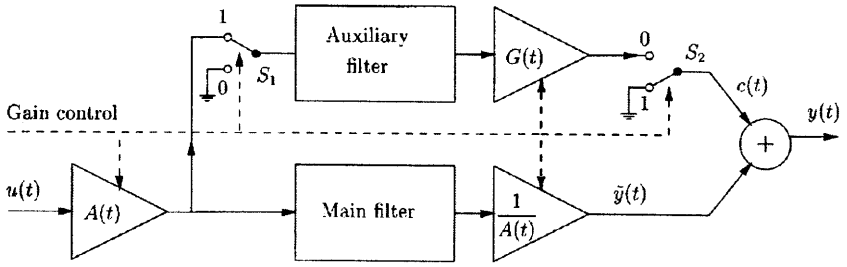

Figure A-1: A corrective signal is added to the system in order to correct for the transients caused by changes in the companding gain level signal. The corrective signal follows Equation A.13 and is generated by two switches and a filter. Both switches are at the top position until a transition occurs in $g[n]$. The switches then flip to the bottom position until $c[n]$ settles to 0 [11].

In the CODEC receiver path, the feed-forward add compensation can only be used for the transient caused by the $\Delta\Sigma$ modulator. The compensation signal must be added in the digital domain, or at the output of the $\Delta\Sigma$ modulator. Compensating for both the $\Delta\Sigma$ modulator and the DCT would require an additional analog adder, which would increase the power needs of the audio path while increase the analog noise in he system. The transient caused by the DCT can be reduced by zero-crossings compensation method discussed in Chapter 5. The system block diagram of this implementation is shown in Figure A-2.

The add compensation method was not tested in simulation because of the complexities of addition after the $\Delta\Sigma$ modulator. In order to add two signals in the $\Delta\Sigma$ domain, an additional $\Delta\Sigma$ modulator would be required, which was determined much too complex for CODEC receiver path.

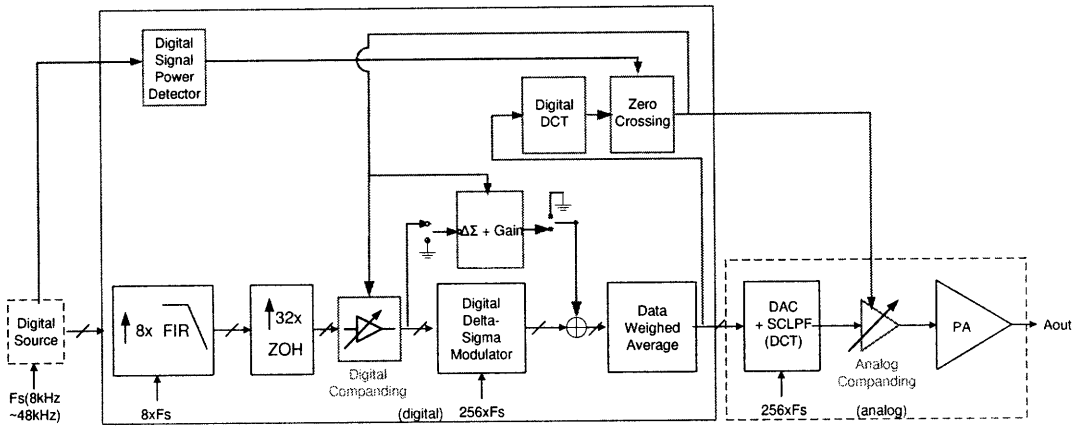

Figure A-2: A corrective signal is added to the receiver path to oppose for the transients caused by changes in the companding gain level signal. The corrective signal follows Equation A.13 and is generated by an auxiliary filter to represent the $\Delta\Sigma$ modulator. The System also implements zero-crossing compensation to eliminate the transients caused by the DCT.

Bibliography

[1] A. B. Clark. Electrical transmitting system, November 1928.

[2] X. Huang D. Lowe. Optimal adaptive hyperbolic companding for ofdm. *2nd Internaltional Conference on Wireless Broadband and Ultra Wideband Communications AusWireless 2007*, 2007.

[3] Y. Tsividis G. Palaskas. Design considerations and experimental evaluation of a syllabic companding audio frequency filter. *Circuits and Systems, 2002. ISCAS 2003. IEEE International Symposium on*, 3:III–305–III308, May 2002.

[4] W.A. Serdiju J. Mulder. A syllabic companding translinear filter. *Circuits and Systems, 1997. ISCAS '97., Proceedings of 1997 IEEE International Symposium on*, 1:101–104, June 1997.

[5] A. Klein and Y Tsividis. Companding digital signal processors. *Proc. 2006 IEEC ICASSP*, 3:III–700–III–703, May 2006.

[6] A. Klein and Y. Tsividis. Instantaenously companding digital signal processors. *IEEE ICASSP*, 3:1433–1436, April 2007.

[7] Y. Tsividis M.T. Ozqun. Dynamic power optimization of active filters with application to zero-if receivers. *Solid-State Circuits, IEEE Journal of*, 41:1344–1352, June 2006.

[8] Bell Telephone Laboratories (Members of the Technical Staff). Transmission systems for communication, 1982.

[9] J. Lee S. Kim. An energy-efficient analog front-end circuit for sub-1v digital hearing aid chip. *Solid-State Circuits, IEEE Journal of*, 41:876–882, April 2006.

[10] B. Smith. Instantaneous companding of quantized signals. *Bell System Technical Journal*, 36:653–709, May 1957.

[11] L. Toth, G. Palaskas, and Y. Tsividis. Two "noninvasive" techniques for syllabic companding in signal processors. *IEEE Transactions on Circuits and Systems II: Analog and Digital Signal Processing*, 48:1085–1098, December 2001.

[12] Y. Tsividis. General approach to signal processors employing companding. *Electronic Letters*, 3:1433–1436, August 1995.

[13] Y. Tsividis. Externally linear, time-invariant systems and their applications to companding signal processors. *IEEE Transactions of Circuits and Systems II*, 44:65–85, February 1997.

[14] L. Toth Y. Tsividis, V. Gopinathan. Companding in signal processing. *Electronic Letters*, 26:1331–1332, August 1990.

[15] N. Krishnapura Y. Tsividis. Internally varying analog circuits minimize power dissipation. *Circuits and Devices Magazine, IEEE*, 19:63–72, January 2003.